



Contents lists available at ScienceDirect

# Bioorganic & Medicinal Chemistry Letters

journal homepage: [www.elsevier.com/locate/bmcl](http://www.elsevier.com/locate/bmcl)

## Optimization of allosteric MEK inhibitors. Part 2: Taming the sulfamide group balances compound distribution properties



Ingo V. Hartung<sup>a,\*</sup>, Stefanie Hammer<sup>b</sup>, Marion Hitchcock<sup>a</sup>, Roland Neuhaus<sup>c</sup>, Arne Scholz<sup>b</sup>, Gerhard Siemeister<sup>b</sup>, Rolf Bohlmann<sup>a</sup>, Roman C. Hillig<sup>d</sup>, Florian Pühler<sup>b</sup>

<sup>a</sup> Medicinal Chemistry, Bayer HealthCare AG, Global Drug Discovery, Muellerstraße 178, 13353 Berlin, Germany

<sup>b</sup> Therapeutic Research Group Oncology, Bayer HealthCare AG, 13353 Berlin, Germany

<sup>c</sup> Research Pharmacokinetics, Bayer HealthCare AG, 13353 Berlin, Germany

<sup>d</sup> Structural Biology, Bayer HealthCare AG, 13353 Berlin, Germany

### ARTICLE INFO

#### Article history:

Received 29 September 2015

Revised 31 October 2015

Accepted 2 November 2015

Available online 3 November 2015

#### Keywords:

Allosteric MEK inhibitor

Oncology

Structure-based drug design

Human carbonic anhydrase

Blood–plasma ratio

### ABSTRACT

Recently, we had identified an unexplored pocket adjacent to the known binding site of allosteric MEK inhibitors which allowed us to design highly potent and *in vivo* efficacious novel inhibitors. We now report that our initial preclinical candidate, featuring a phenoxy side chain with a sulfamide capping group, displayed human carbonic anhydrase off-target activity and species-dependent blood cell accumulation, which prevented us from advancing this candidate further. Since this sulfamide MEK inhibitor displayed an exceptionally favorable PK profile with low brain penetration potential despite being highly oral bioavailable, we elected to keep the sulfamide capping group intact while taming its unwanted off-target activity by optimizing the structural surroundings. Introduction of a neighboring fluorine atom or installation of a methylene linker reduced hCA potency sufficiently, at the cost of MEK target potency. Switching to a higher fluorinated central core reinstated high MEK potency, leading to two new preclinical candidates with long half-lives, high bioavailabilities, low brain penetration potential and convincing efficacy in a K-Ras-mutated A549 xenograft model.

© 2015 Elsevier Ltd. All rights reserved.

After decades of research of the canonical Ras–RAF–MEK–ERK pathway,<sup>1</sup> the BRAF (V600E) inhibitor vemurafenib (Zelboraf<sup>®</sup>, Plexxikon/Roche)<sup>2</sup> and the allosteric MEK inhibitor trametinib (Mekinist<sup>®</sup>, GSK/Japan Tobacco)<sup>3</sup> were recently approved for the treatment of BRAF (V600E) driven metastatic melanoma. Gratifyingly, many years of basic research and drug discovery were finally translated into a significant benefit for patients suffering from one of the deadliest forms of cancer. In addition to being testimony for the advancement of targeted cancer therapeutics, both drug approvals are also prime examples of how first generation clinical development compounds inform many aspects of second generation drug discovery.

Second generation programs are often considered to be less challenging than first generation projects. Quite to the contrary, these projects have to deliver clinical candidates which not only fulfill the traditional PK, PD, safety, toxicological and galenic requirements for clinical development, but in addition have to address specific shortcomings of predecessor compounds. For example, the first generation of advanced clinical MEK1/2

inhibitors, namely PD325901 and AZD6244, did not yield convincing clinical efficacy most likely due to insufficient target engagement.<sup>4</sup> In addition, PD325901 was burdened by ocular toxicity and likely CNS-mediated adverse effects leading to discontinuation of monotherapy clinical studies.<sup>5</sup> In addition, it has been recently reported that activated ERK phosphorylates and inhibits CRAF kinase and that the inhibition of ERK signaling by first-generation allosteric MEK inhibitors, such as PD325901, relieves ERK-dependent feedback inhibition of CRAF and induces MEK phosphorylation in most cells.<sup>6</sup> A new generation of MEK inhibitors, namely GDC-0623 and RO5126766, differ from their predecessors in disrupting this MEK feedback phosphorylation which may translate into superior efficacy.<sup>7</sup>

Taking these findings into account, the second generation of allosteric MEK inhibitors needs to maintain the exquisite target selectivity of its predecessors while surpassing their PK profile, more specifically by reducing brain penetration and at the same time securing continuous target inhibition upon once-daily oral dosing. In addition, effects on MEK feedback phosphorylation have to be monitored.

In our previous communication,<sup>8</sup> we have described the structural evolution of a novel and highly potent series of allosteric

\* Corresponding author.

E-mail address: [ingo.hartung@bayer.com](mailto:ingo.hartung@bayer.com) (I.V. Hartung).

MEK inhibitors. Using PD325901 as a starting point, truncation of its hydroxamic ester headgroup (known to be a metabolic liability) was combined with incorporation of alkyl and aryl ethers at the neighboring C6 ring position (Fig. 1). Whereas alkoxy side chains did not yield inhibitors with sufficient levels of potency, specifically substituted aryloxy groups gave compounds which fulfilled this goal. Sulfamide **1** was identified as a highly potent MEK inhibitor with nanomolar cell potency against BRAF (V600E) as well as Ras-mutated cell lines, high metabolic stability and resulting long half-lives in rodent and non-rodent species. Sulfamide **1** was efficacious in BRAF as well as K-Ras driven xenograft models and, despite being orally bioavailable, displayed a much lower brain/plasma exposure ratio than PD325901.

While fulfilling our target profile for a best-in-class next generation MEK inhibitor, in-depth in vivo profiling of sulfamide **1** in non-rodent species identified a compound-inherent liability which prevented us from further advancing this compound toward clinical development. Additional data for sulfamide **1** and a rational optimization program which culminated in the identification of two new candidates which were devoid of this liability are described in this communication.

Newly synthesized compounds were profiled in an enzymatic COT–MEK cascade assay and in cell proliferation assays employing A375 cells, harboring a BRAF (V600E) mutation, and HCT116 cells, harboring a K-Ras G13D mutation.<sup>9</sup> All presented data are average values of at least two independent measurements. In line with previous publications, A375 cells were found to be significantly more sensitive to MEK inhibition than HCT116 cells.<sup>10</sup> In order not to limit the scope of this program to BRAF-mutated tumor entities, we set the goal of also achieving nanomolar potency in assays with Ras-mutated tumor cell lines.

As reported previously, 6-phenoxy-substituted benzamides with NH-linked functionalities at the 3'-position of the phenoxy side chain have been identified as highly potent MEK inhibitors.<sup>8</sup> Employing a sulfamide capping group, as in compound **1** (Fig. 1, Table 1), provided nanomolar potency even in the less sensitive HCT116 proliferation assay.<sup>11</sup> Sulfamide **1** showed moderate-to-high bioavailabilities in all investigated species (62% in rats, 84% in mice, 85% in dogs) and long half-lives (32 h in rats, 34 h in mice, 58 h in dogs). Most notably, an exceptionally low brain/plasma exposure ratio after iv dosing to mice was found. We have correlated brain/plasma exposure ratios qualitatively to total polar surface area (TPSA) values (as a measure of polarity-driven permeability limitations) and P-glycoprotein (Pgp) recognition (as one well-known mechanism for preventing brain penetration by active efflux).<sup>12</sup> We did not find any evidence of Pgp-mediated efflux of sulfamide **1**; however, analogs from our series with a TPSA value of 130–140 Å<sup>2</sup> consistently possessed low brain penetration potential in mice while retaining sufficient bioavailability after oral dosing.<sup>13</sup>

We were well aware of potential liabilities arising from incorporating an exposed and unsubstituted sulfamide group into our MEK inhibitor lead series. Inhibition of human carbonic anhydrase (hCA) by complexation of its active site Zn<sup>2+</sup> ion with a SO<sub>2</sub>NH<sub>2</sub> group has been known for at least a decade.<sup>14</sup> From a previous clinical program within our company,<sup>15</sup> we were alerted to the fact that binding to hCA may lead to compound accumulation in red blood cells and thereby to exposure variability in patients. Therefore, inhibitory potency in an in vitro hCA assay and blood–plasma ratios were closely monitored for all relevant sulfamide analogs. Sulfamide **1** indeed possessed a submicromolar IC<sub>50</sub> value in our hCA2 assay;<sup>16</sup> however, the blood–plasma ratio in mice (0.6) did not give any initial hint of compound accumulation in red blood cells. Surprisingly, we later learned that sulfamide **1** displayed species-dependent blood–plasma ratios. For non-rodents (dogs, humans), blood–plasma ratios >3 were measured. We did not investigate causes for this species-dependence as we had no rodent CA assay available at that time.

Compound accumulation in red blood cells does not manifest a concern for clinical development per se. However, taking the high potency and long half-life of our candidate into account, and expecting a small therapeutic window for highly potent long-acting MEK inhibitors, we considered the likelihood of interindividual exposure variations in humans due to red blood cell accumulation to be unacceptable for a next generation best-in-class MEK inhibitor.<sup>17</sup> We therefore decided to embark on a further optimization program to remove the unwanted hCA potency while retaining the beneficial characteristics of sulfamide **1** such as submicromolar potency in HCT116 cells, long half-life and low brain penetration potential.

Replacement of the sulfamide group was readily dismissed as a path forward. Sulfamide **1** was originally identified as a metabolite of the dimethylated analog **2** (Table 1).<sup>18</sup> While substituted sulfamides such as **2** (and several analogs with functionalized alkyl substituents; data not shown) were found to be highly potent MEK inhibitors, metabolic instability prevented us from advancing any of these compounds. In general, dealkylation to the mono- or unsubstituted sulfamide group was identified as the dominating metabolic pathway. Thereby, metabolism to pharmacologically active compounds would not only complicate the assessment of PK/PD relationships but ultimately lead back to sulfamide **1** and its hCA issue. Higher alkyl sulfonamides (e.g., compound **3**, Table 1) were found to be as potent as the sulfamide **1** and showed high metabolic stability and long half-lives (e.g., 28 h in rats for ethyl sulfonamide **3**). The lower polarity of sulfonamides versus sulfamides (e.g., TPSA 110.5 Å<sup>2</sup> for **3** vs 136.5 Å<sup>2</sup> for **1**) led to measurable brain exposure levels after iv dosing to mice.

Therefore, we decided to retain the unsubstituted sulfamide moiety of our previous candidate **1** and to tame its undesirable hCA affinity. Initially, we focused our optimization efforts on

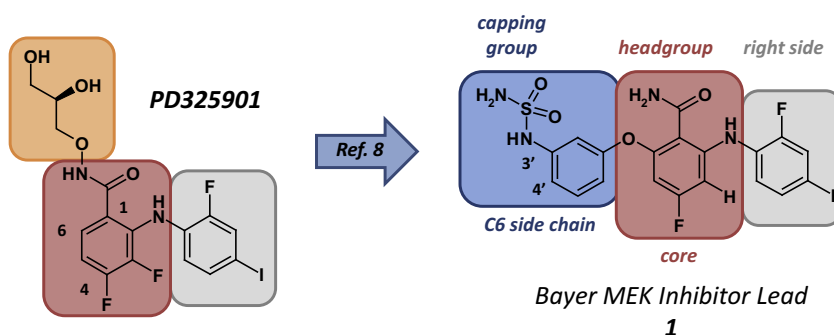
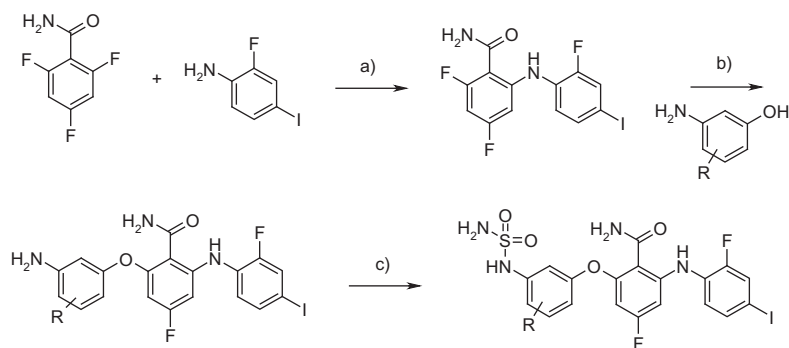


Figure 1. Structural evolution of 6-(aryloxy)benzamide MEK inhibitors.<sup>8</sup>



**Scheme 1.** General synthesis of the sulfamides listed in Table 1. Reagents and conditions: (a) LiHMDS, THF, 0 °C–rt, direct crystallization from crude reaction mixture, 22%; (b) Cs<sub>2</sub>CO<sub>3</sub>, DMF, 50 °C; (c) (i) ClSO<sub>2</sub>NCO, DMAc (cat.), CH<sub>2</sub>Cl<sub>2</sub>, HCO<sub>2</sub>H, 40 °C; (ii) aniline intermediate, DIPEA, DMAc, rt. Abbreviations: DIPEA = diisopropylethylamine, DMAc = dimethylacetamide, LiHMDS = lithium hexamethyldisilazide.

introducing substituents into the neighboring 2'- and 4'-positions to block access of the sulfamide group to the active site Zn<sup>2+</sup> ion of hCA. Sulfamides with substituents adjacent to the sulfamide group were synthesized as described for our initial candidate **1** from 2,4,6-trifluorobenzamide (Scheme 1).<sup>6</sup>

Lithium hexamethyldisilazide promoted nucleophilic substitution allowed introduction of the right-side 2-fluoro-4-iodoaniline. Installation of the second *ortho* substituent was best accomplished by using cesium carbonate as base at slightly increased temperature. In general, high levels of regioselectivity were achieved under these conditions. In most cases, unprotected aminophenols were used which allowed for direct capping with chlorosulfonyl isocyanate in the final step of our synthetic sequence.<sup>19</sup> Our synthetic route was extraordinarily efficient and allowed us to easily screen many commercially available aminophenols as potential linkers.<sup>20</sup> A selection of the newly synthesized analogs is compiled in Table 1 (compounds 4–15).

Introduction of one fluorine atom into the 4'-position (compound **4**) led to a marked drop in target potency. Of note, hCA potency was also significantly reduced and, most importantly, this compound no longer displayed a shift of the mice versus human blood–plasma ratio. Installing a second fluorine atom into the 2'-position (compound **5**) further deteriorated both MEK and hCA potency. Similarly, increasing the size of the 4'-substituent (compounds **6–9**) yielded incremental decreases in MEK potency. Linking the 4'-substituent to the proximal sulfamide nitrogen (compound **10**) did not give rise to a sufficiently potent inhibitor.

Interestingly, moving the blocking substituent from the 4'-position to the 2'-position provided a completely different picture. Installing a methyl group at the 2'-position furnished sulfamide **11**, which was by far the most potent MEK inhibitor in our program at that point in time. Unfortunately, hCA2 potency was unaffected by this substituent which resulted in an unchanged 5-fold shift between mice and human blood–plasma ratios. Larger substituents at the 2'-position (compounds **12** and **13**) paralleled these findings.

Sulfamides **14** and **15** are included in Table 1 as further instructive examples outlining the steepness of structure–activity relationships (SAR) for linker substitutions; we did not expect to influence hCA binding by substituents not adjacent to the sulfamide moiety.

In summary, 4'-fluorinated sulfamide **4** was identified as the most promising new analog with hCA inhibitory potency sufficiently suppressed by the introduced fluoro substituent. While taming the sulfamide, this structural modification at the same time induced an unacceptable deterioration of MEK potency.

As an alternative to introducing neighboring substituents, changing the position of the sulfamide group or introducing methylene groups into the sulfamide appendage were pursued

next (Table 2). All shown analogs were accessible by adopting the general synthetic route as detailed in Scheme 1.

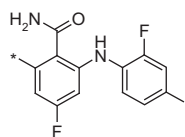
Moving the sulfamide group to the 2'-position (compound **16**) led to a significant drop in enzymatic as well as cellular potency. Of note, hCA2 potency was unaffected by this structural change. Introduction of an additional substituent into the 3'-position (e.g., **17** and **18**) further reduced target potency and thereby did not constitute a viable path forward.

Replacing the inner sulfamide nitrogen of **1** by a methylene group (compound **19**) reduced potency and polarity while affecting hCA2 potency only marginally. Amino sulfonamide **20** was pursued because it retained the desired level of polarity while disrupting the hCA pharmacophore. We were pleased to find that this compound was still a moderately potent MEK inhibitor, although only a micromolar IC<sub>50</sub> value was achieved in the HCT116 proliferation assay. As expected, hCA2 potency was above the upper limit of our assay. Blood and plasma concentrations were closely matched both in mice and humans. Regrettably, compound **20** showed no oral bioavailability in rats, despite being a low clearance compound, most likely due to the marked increase in basicity of the capping moiety and resulting permeability limitations. Benzyl sulfamide **21** showed a much more desirable overall profile with borderline cellular potency, hCA2 activity sufficiently reduced to achieve balanced mouse and human blood–plasma ratios and good PK characteristics (data not shown). Introduction of a methyl group to the benzylic position (compound **22**) was pursued as an option to reinstate higher cellular potency, but failed to be successful. In summary, benzyl sulfamide **21** was identified as an analog being devoid of blood cell accumulation. As for fluoro sulfamide **4**, taming hCA affinity was offset by lower target potency. In turn, the project team now faced the challenge to compensate for the reduced side-chain affinity by optimizing the remainder of the molecule.

Early in our optimization program, variations of the right-side aniline had been pursued without identifying any potency improving modifications. Therefore, we focused on the central benzamide core. Comparing our sulfamides **4** and **21** to PD325901 (Fig. 1) presented us with an immediate option for optimizing the core of our lead series. The additional 3-fluoro substituent of PD325901 had been initially omitted to streamline synthetic access to 6-substituted benzamides. Now, we decided to reintroduce an additional fluoro substituent.

Applying direct CH functionalization to lead compounds (also referred to as *late-stage lead diversification*) has attracted much attention in recent years as an exceptionally efficient way to access new test compounds from already available leads.<sup>21</sup> As a quick entry into higher fluorinated analogs of our MEK inhibitor lead series, we applied direct fluorination conditions (Scheme 2).

**Table 1**  
Blocking strategy to reduce hCA affinity by sterical congestion

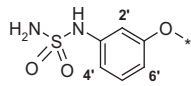
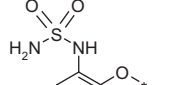
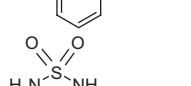
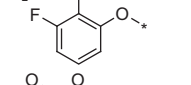
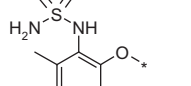
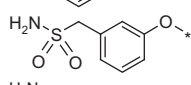
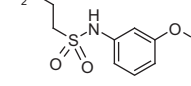
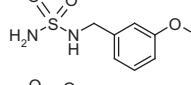


Compound	Side chain	In vitro IC <sub>50</sub> (nM)			TPSA (Å <sup>2</sup> )	hCA2 (μM)	Blood/plasma ratio mouse/human
		MEK1 <sup>a</sup>	A375 (BRAF)	HCT116 (K-Ras)			
1		14	4	180	136.5	0.53	0.6/3.8
2		21	18	155	113.8	–	–
3		15	<30	287	110.5	–	–
4		94	90	2510	136.5	3.8	0.6/0.7
5		118	374	–	136.5	10	–
6		262	180	–	136.5	–	–
7		345	483	–	136.5	–	–
8		592	731	–	145.8	–	–
9		1900	977	–	145.8	–	–
10		127	339	–	137.0	–	–
11		15	2	9	136.5	0.7	1.6/7.6
12		18	6	87	136.5	0.7	1.8/18
13		32	8	152	136.5	–	–
14		899	570	–	–	–	–
15		941	922	–	–	–	–

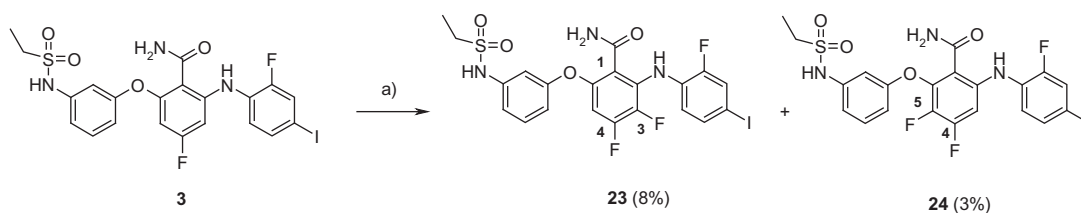
<sup>a</sup> Lower detection limit of this assay: IC<sub>50</sub> of ~5–15 nM.

**Table 2**  
Variation of the sulfamide position and introduction of methylene groups



Compound	Side chain	In vitro IC <sub>50</sub> (nM)			TPSA (Å <sup>2</sup> )	hCA2 (μM)	Blood/plasma ratio mouse/human
		MEK1 <sup>a</sup>	A375 (BRAF)	HCT116 (K-Ras)			
<b>1</b>		14	4	180	136.5	0.53	0.6/3.8
<b>16</b>		81	65	2400	136.5	0.5	—
<b>17</b>		107	138	—	136.5	—	—
<b>18</b>		379	218	—	136.5	—	—
<b>19</b>		32	37	3500	124.5	1.3	—
<b>20</b>		11	88	1800	136.5	>10	2.1/1.6
<b>21</b>		37	35	757	136.5	2.8	0.8/1.1
<b>22</b>		83	24	731	136.5	—	—

<sup>a</sup> Lower detection limit of this assay: IC<sub>50</sub> of ~5–15 nM.



**Scheme 2.** Direct fluorination of ethyl sulfonamide **3**. Reagents and conditions: (a) fluoropyridinium trifluoromethanesulfonate (2 equiv), 1,1,2-trichloroethane, 120 °C.

Ethyl sulfonamide **3** was selected as starting material because we had gram quantities available and did not expect interference of fluorinating reagents by the sulfonamide group. Gratifyingly, we were able to isolate both regioisomeric difluorinated benzamide cores from a single fluorination reaction. On first inspection, the isolated yields of 8% (**23**: 3,4-F<sub>2</sub> core) and 3% (**24**: 4,5-F<sub>2</sub> core) may be considered unacceptably low; however, it must be taken into account that this approach allowed us to assess both new cores within days instead of embarking on multistep route synthetic endeavors. Thereby, the benefits clearly outweighed the disadvantage of low isolated yields.<sup>22</sup>

**Table 3**  
Influence of the core fluorination pattern on potency

Compound	In vitro IC <sub>50</sub> (nM)		
	MEK1 <sup>a</sup>	A375 (BRAF)	HCT116 (K-Ras)
<b>3</b>	15	<30	287
<b>23</b>	12	2.4	65
<b>24</b>	15	4	81

<sup>a</sup> Lower detection limit of this assay: IC<sub>50</sub> of ~5–15 nM. For structures of compounds **23** and **24**, see [Scheme 2](#).

As can be seen from Table 3, introduction of the second fluorine substituent into the core of **3** increased cellular potency more than 4-fold (e.g., IC<sub>50</sub> 60–80 nM vs 287 nM in the HCT116 cell proliferation assay). The sulfonamide with the corresponding 3,4,5-trifluorinated core was found to be almost as potent as **23** and **24** with the difluorinated cores (data not shown). Further profiling in PK assays identified the 3,4-difluorinated core (as in sulfonamide **23** and in PD325901) as the most promising core. Therefore, we decided to combine this difluorinated core with our preferred side chains.

Several synthetic routes were pursued for these new target compounds. Adopting our previously used general route (Scheme 1) necessitated using 2,3,4,6-tetrafluorobenzamide as starting material. Unfortunately, base-promoted introduction of phenols was not ortho-selective, as before. Instead, the additional 3-fluoro substituent activated the fluorine atom at the 4-position, thereby leading to not readily separable mixtures of regioisomers with the desired regioisomer as only the minor component. Therefore, a more efficient and selective route was needed. One solution to circumvent the regioselectivity issue is outlined in Scheme 3.

In order to capitalize on hidden symmetry, we employed 3,4,5-trifluorophenylboronic acid as starting material and changed the order of side-chain installations. First, the C6 side chain was introduced by an Ullmann-type coupling of the phenol with the boronic acid in the presence of copper(II) acetate. Subsequent metalation and CO<sub>2</sub> quenching installed the C1 carboxylic acid group. Introduction of the aniline side chain under basic conditions delivered the desired *N*-arylaniline, albeit in low isolated yield.<sup>23</sup> Transformation of the carboxylic acid into the corresponding benzamide and final Boc deprotection delivered the target compound **28**. Data for compounds containing the combination of the 3,4-difluoro core with preferred and most instructive C6 side chains are compiled in Table 4.

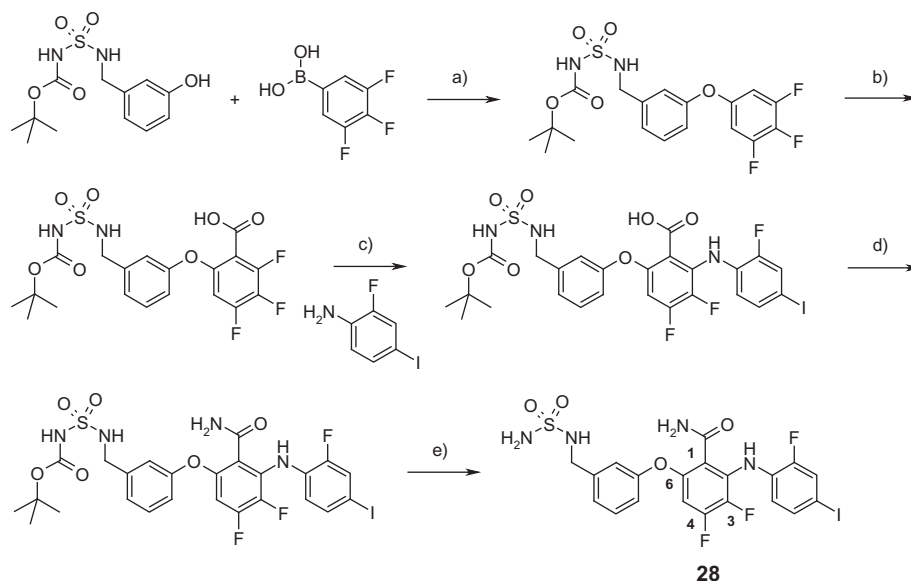
Combining the improved core with the unchanged sulfamide side chain of our previous candidate 1 provided the expected gain in antiproliferative potency. Several of the newly synthesized analogs reached the lower detection limit of the biochemical MEK assay (IC<sub>50</sub> values below 20 nM). Therefore the true difference in potency between those analogs became only apparent by compar-

ing cellular potency data. Already established SAR trends for side chains were unaffected by switching to the higher fluorinated core (e.g., compound **26** being equally potent to compound **25**). Most importantly, employing the 4'-fluorophenyl sulfamide side chain or the benzyl sulfamide side chain provided us with two compounds (**27** and **28**) which fulfilled our optimization goals. Antiproliferative potency was once again in the range of our previous candidate (compare to Table 1). In addition, hCA2 potency was reduced for both compounds **27** and **28** by 10-fold relative to 1, which translated into balanced human and mouse blood–plasma ratios. Compounds **29** and **30** showcase that we were able to counterbalance reduced side-chain affinity in several, but not all, cases by the higher fluorinated core. Sulfamide **31** was finally prepared for solely academic reasons to prove the additivity of potency-increasing effects: By combining the most potent side chain (analog **11**, Table 1) with the most potent core (compound **23**, Scheme 2), we achieved an IC<sub>50</sub> of 2 nM in the HCT116 proliferation assay, which is 100-fold more potent than our previous candidate 1 and PD325901.

Compounds from this series of allosteric MEK inhibitors as well as hybrids between our series and published MEK inhibitors were investigated with regard to their effects on MEK feedback phosphorylation and were found to differ significantly from the first generation of MEK inhibitors, namely PD325901. These results and a discussion of structural features likely responsible for modulating MEK feedback phosphorylation will be reported elsewhere.<sup>24</sup>

Nevertheless, for advanced optimization projects, potency is rarely the decisive selection criterion as was the case in our project where sulfamides **27** and **28** were selected based on their overall most favorable profile.

Since our novel sulfamides **27** (BAY-866) and **28** (BAY-438) were unchanged with respect to overall polarity and we had not introduced new metabolic liabilities, we did not expect major changes in their PK profiles compared to our previous candidate 1. Indeed, both new sulfamides showed the same favorable PK profile as their predecessor (Table 5) with low clearance, long half-life and high bioavailability in rats. In addition, no relevant compound exposure was seen in brain tissue after iv dosing to mice.



**Scheme 3.** Synthesis of sulfamide **28** with a 3,4-difluorinated benzamide core. Reagents and conditions: (a) Cu(OAc)<sub>2</sub> (1 equiv), pyridine, rt, 20%; (b) LDA (5.5 equiv), CO<sub>2</sub> (excess), –78 °C–rt, 61%; (c) LiHMDS (7.5 equiv), THF, 0 °C, 19%; (d) CDI, NH<sub>3</sub>, DMF, rt, 36%; (e) TFA, CH<sub>2</sub>Cl<sub>2</sub>, rt, 85%. Abbreviations: CDI = 1,1'-carbonyldiimidazole, LDA = lithium diisopropylamide, LiHMDS = lithium hexamethyldisilazide, TFA = trifluoroacetic acid.

**Table 4**

Compounds containing a difluorinated benzamide core with a preferred C6 side chain



Compound	Side chain	In vitro IC <sub>50</sub> (nM)			TPSA (Å <sup>2</sup> )	hCA2 (μM)	Blood/plasma ratio mouse/human
		MEK1 <sup>a</sup>	A375 (BRAF)	HCT116 (K-Ras)			
<b>25</b>		13	2	50	136.5	–	–
<b>26</b>		10	6	42	113.6	–	–
<b>27</b> BAY-866		14	13	277	136.5	4.6	0.8/1.0
<b>28</b> BAY-438		21	4	124	136.5	5	0.8/0.8
<b>29</b>		22	11	303	124.5	2.2	0.8/1.1
<b>30</b>		28	32	2950	136.5	–	–
<b>31</b>		14	0.2	2	136.5	–	–

<sup>a</sup> Lower detection limit of this assay: IC<sub>50</sub> of ~5–15 nM.**Table 5**

PK data of key compounds

Compound	Rat PK <sup>a</sup>				Mice PK
	Cl <sub>blood</sub> (L/kg/h)	V <sub>ss</sub> (L/kg)	t <sub>1/2</sub> (h)	F (%)	Brain/plasma ratio <sup>b</sup>
PD325901	0.5	1.7	5.4	104	0.11
AZD6244	0.06	0.2	4.1	24	<0.02
<b>1</b>	0.03	2.0	32	62	<0.02
BAY-866 ( <b>27</b> )	0.02	0.5	26	84	<0.02
BAY-438 ( <b>28</b> )	0.07	1.9	32	78	<0.02

<sup>a</sup> Dosing for PD325901: 0.5 mg/kg iv/1 mg/kg po; dosing for AZD6244: 0.5 mg/kg iv/5 mg/kg po; dosing for **1**: 1 mg/kg iv/1 mg/kg po; dosing for **27** and **28**: 0.5 mg/kg iv/1 mg/kg po.<sup>b</sup> AUC(brain)/AUC(plasma) for 0–3 h after 5 mg/kg iv dosing.

As for our previous candidate **1**, we did not identify any proof of Pgp-mediated active efflux in pharmacokinetic (e.g., Caco-2 assay) or pharmacological studies as a reason for the low brain penetration behavior. For example, pERK inhibition measurements in a matched pair of cell lines (HeLa-MaTu vs the Pgp-expressing HeLa-MaTu-ADR cell line) showed a significant IC<sub>50</sub> shift for AZD6244 (3.7 μM in HeLa-MaTu-ADR vs 14 nM in HeLa-MaTu), proving that AZD6244 is a strong Pgp substrate which prevents access across the blood–brain barrier. For PD325901, low nanomolar IC<sub>50</sub> values for pERK inhibition were measured in both cell lines. Our novel sulfamides BAY-866 and BAY-438 closely matched the profile of PD325901, with a smaller than 5-fold shift in IC<sub>50</sub> values between the two cell lines (e.g., 1.8 nM in HeLa-MaTu and 8.7 nM in HeLa-MaTu-ADR for sulfamide **28**). At the same time, both

**Table 6**

Cell proliferation data of key compounds

Compound	IC <sub>50</sub> (nM)					
	A375 (BRAF)	COLO205 (BRAF)	HepG2 (N-Ras)	HCT116 (K-Ras)	A549 (K-Ras)	MCF7
PD325901	13	5	5	185	166	9550
AZD6244	31	69	32	3000	1750	>10,000
BAY-866 ( <b>27</b> )	13	42	2	277	314	>10,000
BAY-438 ( <b>28</b> )	4	9	5	124	185	>10,000

sulfamides showed significantly lower brain penetration behavior than PD325901 in mice iv dosing studies (Table 5). This likely reflects the higher polarity and higher hydrogen bond donor count of **27** and **28** and thereby impaired passive diffusion via the blood–brain barrier, which is known to be more restrictive to polar compounds than the GI barrier.<sup>25</sup>

Our two new candidates were subsequently profiled in a larger panel of cell lines (see Table 6 for a selection of the data). Benzyl sulfamide BAY-438 (**28**) was as potent as PD325901, while the 4'-fluorophenyl sulfamide BAY-866 (**27**) was slightly less potent. As expected, no antiproliferative activity was seen in cell lines devoid of Ras–RAF–MEK–ERK pathway deregulation. In line with these findings, we did not see relevant off-target activities in selectivity panels (e.g., kinase panels).

Both novel sulfamides showed strong efficacy in A549 mice xenograft studies (Fig. 2). In line with our in vitro data, BAY-438

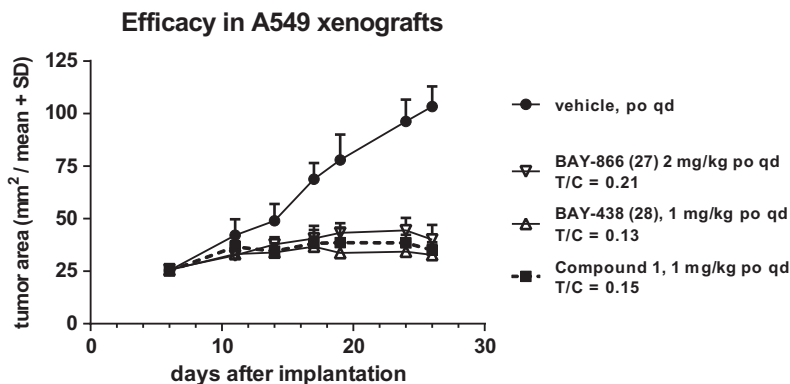


**Figure 2.** In vivo A549 xenograft study with sulfamides BAY-866 (**27**) and BAY-438 (**28**) in nude mice.

was slightly more potent (maximal efficacy reached @ 1 mg/kg oral daily dosing) than BAY-866 (2 mg/kg orally once daily).

In conclusion, we were able to tame hCA potency of sulfamide-containing allosteric MEK inhibitors by structural changes in the direct vicinity of the sulfamide group. State-of-the-art MEK potency was subsequently reinstated by introducing an additional fluorine atom into the central benzamide core. A streamlined compound profiling tree with high predictability of pharmacological and PK in vitro assays for in vivo performance, in combination with short and flexible synthetic routes, secured fast learning cycles. This enabled selection of two new preclinical candidates within 6 months after identification of the hCA liability of the initial candidate. Both candidates fulfilled the target profile for next generation allosteric MEK inhibitors. Both compounds have been advanced to non-rodent safety and toxicological profiling.

## References and notes

- (a) Roberts, P. J.; Der, C. J. *Oncogene* **2007**, *26*, 3291; (b) Montagut, C.; Settleman, J. *Cancer Lett.* **2009**, *283*, 125.
- Bollag, G.; Tsai, J.; Zhang, J.; Zhang, C.; Ibrahim, P.; Nolop, K.; Hirth, P. *Nat. Rev. Drug Disc.* **2012**, *11*, 873.
- (a) Gilmartin, A. G.; Bleam, M. R.; Groy, A.; Moss, K. G.; Minthorn, E. A.; Kulkarni, S. G.; Rominger, C. M.; Erskine, S.; Fisher, K. E.; Yang, J.; Zappacosta, F.; Annan, R.; Sutton, D.; Laquerre, S. G. *Clin. Cancer Res.* **2011**, *17*, 989. See also: (b) Abe, H.; Kikuchi, S.; Hayakawa, K.; Iida, T.; Nagahashi, N.; Maeda, K.; Sakamoto, J.; Matsumoto, N.; Miura, T.; Matsumura, K.; Seki, N.; Inaba, T.; Kawasaki, H.; Yamaguchi, T.; Kakefuda, R.; Nanayama, T.; Kurachi, H.; Hori, Y.; Yoshida, T.; Kakegawa, J.; Watanabe, Y.; Gilmartin, A. G.; Richter, M. C.; Moss, K. G.; Laquerre, S. G. *ACS Med. Chem. Lett.* **2011**, *2*, 320.
- In the meantime, AZD6244 has been moved into phase III studies for the treatment of K-Ras-mutated NSCLC in combination with docetaxol, after identification of a superior compound formulation.
- Haura, E. B.; Ricart, A. D.; Larson, T. G.; Stella, P. J.; Bazhenova, L.; Miller, V. A.; Cohen, R. B.; Eisenberg, P. D.; Selaru, P.; Wilner, K. D.; Gadgeel, S. M. *Clin. Cancer Res.* **2010**, *16*, 2450.
- (a) Hatzivassiliou, G.; Haling, J. R.; Chen, H.; Song, K.; Price, S.; Heald, R.; Hewitt, J. F. M.; Zak, M.; Peck, A.; Orr, C.; Merchant, M.; Hoeflich, K. P.; Chan, J.; Luoh, S.-M.; Anderson, D. J.; Ludlam, M. J. C.; Wiesmann, C.; Ultsch, M.; Friedman, L. S.; Malek, S.; Belvin, M. *Nature* **2013**, *501*, 232; (b) Ishii, N.; Harada, N.; Joseph, E. W.; Ohara, K.; Miura, T.; Sakamoto, H.; Matsuda, Y.; Tomii, Y.; Tachibana-Kondo, Y.; Iikura, H.; Aoki, T.; Shimma, N.; Arisawa, M.; Sowa, Y.; Poulikakos, P. I.; Rosen, N.; Aoki, Y.; Sakai, T. *Cancer Res.* **2013**, *73*, 4050.
- Caunt, C. J.; Sale, M. J.; Smith, P. D.; Cook, S. J. *Nat. Rev. Cancer* **2015**, *15*, 577.
- Hartung, I. V.; Hitchcock, M.; Pühler, F.; Neuhaus, R.; Scholz, A.; Hammer, S.; Petersen, K.; Siemeister, G.; Brittain, D.; Hillig, R. C. *Bioorg. Med. Chem. Lett.* **2013**, *23*, 2384.
- For detailed assay descriptions, see: (a) Rudolph, J.; Dumas, J.; Li, Y.; Auclair, D.; Lobell, M.; Hitchcock, M.; Hartung, I.; Koppitz, M.; Brittain, D.; Pühler, F.; Petersen, K.; Guenther, J. PCT Patent WO 2008/138639; (b) Hitchcock, M.; Hartung, I. PCT Patent WO 2009/129938.
- Solit, D. B.; Garraway, L. A.; Pratilas, C. A.; Sawai, A.; Getz, G.; Basso, A.; Ye, Q.; Lobo, J. M.; She, Y.; Osman, I.; Golub, T. R.; Sebolt-Leopold, J.; Sellers, W. R.; Rosen, N. *Nature* **2006**, *439*, 358.
- Cell proliferation inhibition data were correlated in selected cases to measurements of pERK inhibition in the respective cell lines (Mesoscale assay set-up) to rule out off-target cytotoxicity. As pERK inhibition  $IC_{50}$  values in general paralleled proliferation  $IC_{50}$  values the former are—for the sake of clarity—excluded from this manuscript.
- (a) Bagal, S. K.; Bungay, P. J. *ACS Med. Chem. Lett.* **2012**, *3*, 948; (b) Di, L.; Rong, H.; Feng, B. *J. Med. Chem.* **2013**, *56*, 2.
- Traditionally, a TPSA value of  $120 \text{ \AA}^2$  is considered to be a cut-off for securing sufficient passive diffusion through the GI barrier. In the case of sulfamide **1** and related analogs, intramolecular hydrogen bonds between the amide headgroup and the neighboring ether and amine linkages have to be taken into account as they reduce the exposed polar surface area. Therefore, we have not compared TPSA data to compounds which do not feature this intramolecular H-bonding network, for example, PD325901.
- Ceruso, M.; Vullo, D.; Scozzafava, A.; Supuran, C. T. *Bioorg. Med. Chem.* **2013**, *21*, 6929, and references cited therein.
- Lücking, U.; Jautelat, R.; Krüger, M.; Brumby, T.; Lienau, P.; Schäfer, M.; Briem, H.; Schulze, J.; Hillisch, A.; Reichel, A.; Wengner, A. M.; Siemeister, G. *ChemMedChem* **2013**, *8*, 1067.
- Inhibitory potency against human carboanhydrase isozymes 1 (hCA1) closely paralleled data for hCA2, albeit at a lower potency level (e.g.,  $IC_{50}$  4.8  $\mu\text{M}$  for sulfamide **1**). For the sake of clarity, hCA1 data are omitted from this manuscript.
- Sulfamide-containing dual Raf–MEK inhibitors based on a coumarin core were reported recently by researchers from Chugai without any mention of hCA findings: Aoki, T.; Hyohdoh, I.; Furuichi, N.; Ozawa, S.; Watanabe, F.; Matsushita, M.; Sakaitani, M.; Ori, K.; Takanashi, K.; Harada, N.; Tomii, Y.; Tabo, M.; Yoshinari, K.; Aoki, Y.; Shimma, N.; Iikura, H. *Bioorg. Med. Chem. Lett.* **2013**, *23*, 6223.
- Identification of clinical candidates as metabolites of initial lead compounds, a process which has been coined as pre-metabolization, is not uncommon in lead optimization programs: Clader, J. W. *J. Med. Chem.* **2004**, *47*, 1.
- In selected cases, tert-butoxycarbonyl-protected aminophenols were used, with subsequent deprotection under acidic conditions.
- Gratifyingly, aniline intermediates (devoid of the sulfamide capping group) could already be used for SAR assessment. MEK inhibitory potency trends for aniline intermediates paralleled SAR for the fully functionalized sulfamides (data not shown), albeit on a lower potency level. Thereby, we were able to screen many more aminophenols than indicated in Tables 1 and 2 and discard low potency linkers already at the aniline intermediate step.
- (a) Wencel-Delord, J.; Glorius, F. *Nat. Chem.* **2013**, *5*, 369; (b) Masood, M. A.; Bazin, M.; Bunnage, M. E.; Calabrese, A.; Cox, M.; Fancy, S.-A.; Farrant, E.; Pearce, D. W.; Perez, M.; Hitzel, L.; Peakman, T. *Bioorg. Med. Chem. Lett.* **2012**, *22*, 1255.
- In general, we consider an isolated yield of 10% in a final-stage-diversification reaction as a more than acceptable outcome as this yield equates to a eight-step sequence with 75% yield for each individual step, while reducing time and resource investments by more than 95%.
- The low isolated yield did not result from low regioselectivity of the addition reaction but rather from low product recovery upon column chromatographic purification due to limited solubility in organic solvents.
- Hartung, I. V.; Pühler, F.; Neuhaus, R.; Scholz, A.; Siemeister, G.; Geisler, J.; Hillig, R. C.; von Ahsen, O.; Hitchcock, M. *ChemMedChem* **2015**, in press.
- Wager, T. T.; Hou, X.; Verhoest, P. R.; Villalobos, A. *ACS Chem. Neurosci.* **2010**, *1*, 435.